J Mater Sci (2008) 43:1121–1127
DOI 10.1007/s10853-007-2271-9

Prediction of the effect of artificial aging heat treatment on the yield strength of an open-cell aluminum foam

Daniel R. A. Cluff · Shahrzad Esmaeili

Received: 22 December 2006 / Accepted: 29 October 2007 / Published online: 4 December 2007

Abstract The effect of artificial aging on the compression yield strength of an open-cell AA6101 foam is studied using both experimental and modeling approaches. Isothermal calorimetry is used to analyze the precipitation kinetics of the foam. The modeling work combines the established approaches for predicting the yield strength of open-cell metallic foams as a function of the relative density and normalized strength, as well as the age hardening behavior of AA6101 alloy. The foam yield strength is related to the evolution of precipitate content during aging and is modeled for artificial aging at 180 and 220 °C. It is shown that the model predictions match very well with the experimentally determined yield strength values. The overall results suggest that the presented analytical and modeling approaches can effectively be used to predict the precipitation hardening behavior and/or optimize processing and properties of AA6101 foams.

Introduction

Aluminum foams are among the new engineering materials with numerous desirable properties such as high specific strength and stiffness, energy absorption, and damping capacity [1–6]. These properties create great potential for aerospace applications, as well as lightweighting and crashworthiness in the new generation of passenger cars and transportation vehicles. There have been numerous investigations on the processing, characterization, properties, and performance of metallic foams in the past 25 years, which have provided a wealth of knowledge on these advanced materials [e.g. 1–20]. The analysis of the deformation mechanisms in cellular solids by Gibson and Ashby in early 1980s [e.g. 7] have yielded simple modeling formulations relating the relative density to normalized mechanical properties of foams. These models have become widely accepted in the analysis of the mechanical behavior of cellular materials since then [1, 2, 8–16]. The model that relates the compressive yield strength of an elastic–plastic foam to its relative density is given as follows [1]:

$$\frac{\sigma^*_{pl}}{\sigma_{YS}} = C\left(\frac{\rho^*}{\rho_s}\right) \tag{1}$$

where σ^*_{pl} is the plastic collapse strength (i.e. yield strength) of the foam and σ_{YS} the yield strength of the cell wall material. C is the proportionality constant related to cell geometry, and found to be approximately 0.3 for a wide-range of open-cell metallic foams [1, 2]. The two parameters ρ^* and ρ_s are the densities of the foam and the solid cell-wall material, respectively. The influence of heat treatment on the compressive strength of aluminum foams has been investigated by various researchers. Lehmus et al. [6, 17, 18] have reported that age hardening of as-fabricated and solution treated foam specimens results in significant increase in the compressive strength of closed cell AA6XXX and AA7XXX foams. Similarly, Chan and Chan [19] have found that age hardening treatments significantly increase the compressive yield strength of closed-cell SiC particle reinforced A356 and open-cell AA6061 foams. However, the ductility reduces and the failure mode changes from ductile to brittle in the age hardened AA6061 foam [19]. Zhou et al. [20] have studied

D. R. A. Cluff · S. Esmaeili (✉)
Department of Mechanical and Mechatronics Engineering, University of Waterloo, 200 University Ave. West, Waterloo, ON, Canada N2L 3G1
e-mail: shahrzad@uwaterloo.ca

the effect of heat treatment on the compressive deformation behavior of open-cell Duocel® AA6101 foam. Their results also indicate that solution treated and artificially age hardened (i.e. T6 temper) foam attains a higher level of strength compared to the as-fabricated or annealed tempers of the foam. Despite these efforts in establishing the effect of age hardening heat treatments on strengthening of various aluminum foams, the precipitation hardening behavior of foams has not been effectively modeled. The present work aims at providing a predictive tool that relates the yield strength of an open-cell AA6101 foam to its microstructural evolution during age hardening processes. The microstructural evolution of the foam is studied using the isothermal calorimetry procedure introduced by Esmaeili et al. [21]. The results of the calorimetry experiments are used to determine the precipitation kinetics of the foam material using the Johnson-Mehl, Avrami and Kolmogorov (JMAK) approach [22]. The kinetic parameters are then used to model the yield strength of the foam by combining Eq. 1 with the yield strength model developed by Esmaeili et al. [22]. The model predictions are validated using the results of compression tests on age-hardened foams.

Experimental procedure

Open-cell Duocel® 6101 Aluminum foam, with a pore size of 10 ppi (i.e. pores per inch) and a nominal relative foam density of 6–8%, is used in this investigation. The ASM Handbook gives the nominal (maximum) alloying element content of the alloy as: 0.1 wt% Cu, 0.35–0.8 wt% Mg, and 0.30–0.70 wt% Si [23]. The as-fabricated foam blocks are obtained from ERG Materials and Aerospace Corporation, Oakland. Test samples are cut from the foam blocks using a band saw.

The heat treatment of foam samples includes solution treatment in an air furnace at 560 °C for 1 h, followed by air quenching to room temperature and subsequent aging treatments in an air atmosphere. Age hardening treatments are conducted in the temperature range of 180–220 °C, due to the relevance of these temperatures to commercial artificial aging treatments of AA6XXX bulk alloys and foams [e.g. 20, 21]. Although quenching in air is not as fast as water quenching and may result in the loss of solutes to grain boundary precipitation, this quenching procedure is selected to reduce the time delay between the quenching and aging practices. This is particularly important considering that the isothermal calorimetry samples should not have water residue (from the water quenching practice) when the test starts. Therefore, air quenching eliminates the need for sample drying prior to the calorimetry tests. In the present work, the time that a sample is kept at room temperature after air quenching and prior to the start of aging treatment is less than 2 min. It should be noted that the yield strength values obtained in the present age hardened foams might be smaller than the values reported in the literature for the commercially heat treated Duocel® foam samples, due to the selected solutionizing and quenching procedure.

Isothermal calorimetry tests are conducted using a SETARAM C80 Calorimeter. Samples of 5 × 5 × 40 mm (approximately 870 mg) are used for this purpose. Calorimetry tests, which represent artificial aging treatments, are conducted at 180, 200 and 220 °C for durations corresponding to the overaged conditions of the alloy (up to 20 h). The calorimeter, with empty test and reference vessels, is allowed to stabilize at the test temperature before starting data acquisition. The test run then starts by opening the test vessel's lid and dropping the solution treated and quenched sample into the test vessel, while the reference vessel is kept empty. This sample introduction method creates an initial destabilization of the calorimeter and a large endothermic effect at the start of the test, both of which are corrected using baseline runs [24]. In order to obtain the baseline trace at the test temperature for a foam sample, a second test is conducted on the sample which has overaged during the first test run at that temperature. The same data acquisition parameters and sample drop procedure are used for this second run. The result of the baseline run is then subtracted from the result of the test run and an appropriate time shift is applied for the correction of the initial calorimeter disturbance [24]. The calorimetry tests are repeated at least three times at each test temperature to ensure repeatability of the results.

The foam samples for compression testing are cut into rectangular-based blocks of approximately 44.0 × 44.0 × 50.8 mm with the long dimension in the direction of cell orientation. These dimensions are chosen to ensure that sample size effects are eliminated by having at least eight cells in each direction [1, 25]. The sample dimensions are measured with digital calipers to an accuracy of 0.1 mm. The mass of each sample is recorded to an accuracy of 0.0005 g for calculation of the foam density. The relative density (i.e. $\frac{\rho^*}{\rho_s}$) is calculated by dividing the foam density by the density of aluminum (i.e. 2.8 g/cm^3). The relative density values vary between 7.4 and 7.5%. As noted in Section "Modeling of the yield strength", the latter is chosen in using Eq. 1 for modeling of the foam strength. Samples are aged for 1, 2, 4, and 7 h at 180 °C and 0.5, 1, 1.5, 2, and 4 h at 220 °C prior to compression testing. The samples are compressed in the direction of the overall cell elongation using an Instron 4205 machine fitted with a 15,000 Kgf load cell. Crosshead speed during compression is 20 mm/min. Testing is halted when the load reaches 7,000 Kgf. Although for the current analysis only the yield stress values are required, this ensures deformation beyond

foam densification and allows the full stress–strain behavior to be studied. The tests are performed at least two times for each aging condition, with a majority of them repeated three times, to ensure repeatability of the stress–strain curves.

Experimental results and modeling analysis

Isothermal calorimetry

The results of the isothermal calorimetry tests at 180, 200, and 220 °C are shown in Fig. 1. Exothermic heat effects, i.e. $\frac{dQ}{dt}$ (in mW/mg), which rapidly rise to maximum values and then slowly reduce to the baseline levels of the calorimeter are observed in each case. Following the reports on the precipitation hardening behavior of AA6XXX alloys, the time to reach the baseline level of the heat effect (i.e. "zero heat effect") during artificial aging is considered as the peak-aged condition [21, 22, 24, 26]. These times, i.e. t_{peak}, are measured as 10 h at 180 °C, 5 h at 200 °C, and 4 h at 220 °C. The integrated areas under the isothermal traces up to the peak-aged conditions, i.e. $\int_0^{t_{peak}} \frac{dQ}{dt} dt$, are measured as approximately 5.4 J/g for 180 °C, 3.7 J/g for 200 °C, and 4.1 J/g for 220 °C. Considering all the experimental, as well as the measurement errors [22, 24], these values are very similar. This finding suggests that the foam alloy, as in the case of AA6111 alloy [21, 22], has similar precipitate contents for the peak-aged conditions in the temperature range of 180–220 °C. The evolution of the relative volume fraction of precipitates, i.e. f_r, is estimated using the following equation [21]:

$$f_r = \frac{\int_0^t \frac{dQ}{dt} dt}{\int_0^{t_{peak}} \frac{dQ}{dt} dt} \quad (2)$$

where t is the aging time. These experimentally estimated results for f_r at different temperatures are shown in Fig. 2. Typical curves, representing the kinetics of precipitation in AA6XXX alloys [21, 22], are obtained. The precipitation rate in each case is initially rapid and then slowly decreases with aging time.

It has been shown that the evolution of the precipitate volume fraction during artificial aging of as-quenched AA6XXX alloys can be approximated using the JMAK kinetic model as follows [e.g. 22, 26]:

$$f_r = 1 - \exp(-kt^n) \quad (3)$$

where k (in s^{-n}) and n (dimensionless) are the kinetic parameters. Equation 3 is fitted to the experimental results obtained from the analysis of the isothermal calorimetry traces according to Eq. 2. The kinetic parameters are obtained by the conventional procedure of fitting a straight line to the experimental $\ln \ln \left(\frac{1}{1-f_r}\right)$ vs. $\ln t$ data and finding the slope (i.e. n) and the y-intercept (i.e. $\ln(k)$) of the fitted line in the f_r range of 0.05–0.95 [26]. Similar to the results on other AA6XXX alloys [22, 26, 27], it is found that $n \cong 1$ for all the three temperatures. Table 1 lists the values

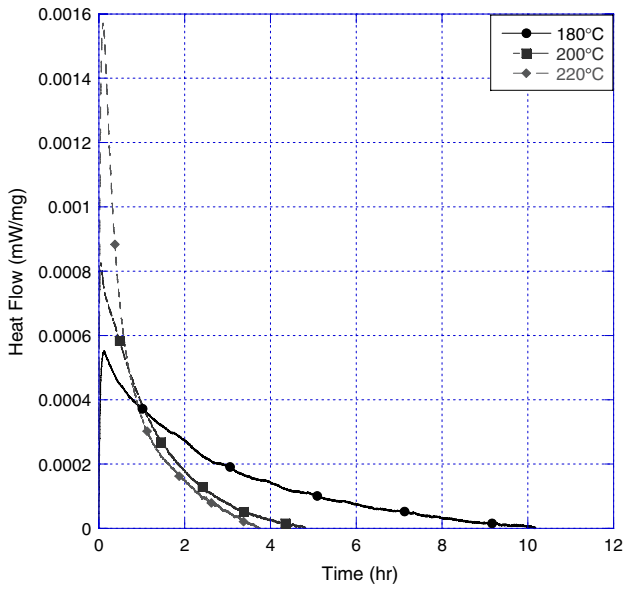

Fig. 1 Results of the isothermal calorimetry tests on foam samples at 180, 200, and 220 °C

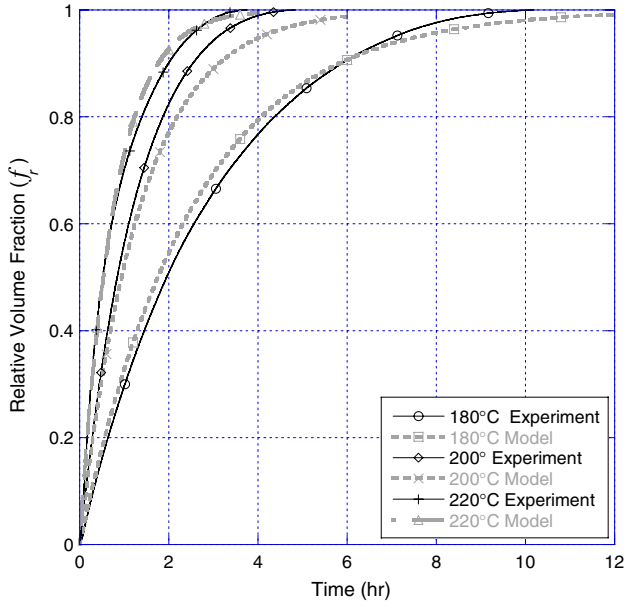

Fig. 2 Evolution of the relative volume fraction of precipitates in the foam samples during aging at 180, 200, and 220 °C

Table 1 JMAK kinetic parameters

Temperature (°C)	n	k (s^{-1})	R^2
180	1	1.05E-04	0.995
200	1	2.30E-04	0.994
220	1	3.60E-04	0.994

obtained for k and n along with the correlation coefficient (R^2) at each temperature. These values are used to obtain the temperature dependence of k according to the Arrhenius relationship as follows [22]:

$$k = k_0 \exp\left(\frac{-Q_A}{RT}\right) \quad (4)$$

where Q_A is an apparent activation energy in kJ/mol, T is the temperature in Kelvin and R is the universal gas constant. The plot of $\ln(k)$ vs. $\frac{1}{T}$, which yields $Q_A \cong 57$ kJ/mol and $k_0 \cong 457\ s^{-1}$, is shown in Fig. 3. The values obtained for n, Q_A, k_0 are used to predict the evolution of the volume fraction of precipitates during artificial aging of the foam material according to JMAK kinetic model. The predicted values of f_r are shown in Fig. 2 for direct comparison with the values obtained from calorimetry data (i.e. Eq. 2).

Compression testing

Compression testing results showed typical stress–strain curves previously reported for plastic foams in general [1] and the Duocel® foam in particular [20]. A representative result from an underaged foam, showing schematic elastic–plastic (I), plastic (II), and full densification (III) regimes, is shown in Fig. 4. The yield strength of the foam, which occurs in the boundary region overlapping regimes (I) and (II), is taken as the maximum (i.e. upper yield) stress if the curve displays a "stress peak and valley" as a result of yielding [20]. If the curve does not display such a distinctive yielding, and rather a gradual increase in stress with strain is observed, the stress at a strain of 0.05 is taken as the yield strength [6]. It should be noted that the average value of the measured yield strengths for each aging condition is reported in this work and the variation of 1–15% between the measured and average values have been recorded for the tested aging conditions. This variation was significantly lower than the aging response of the as-quenched foam at any aging condition. The average yield strength values are used to validate the predictions of the foam yield strength, as presented in Sect. "Modeling of the yield strength".

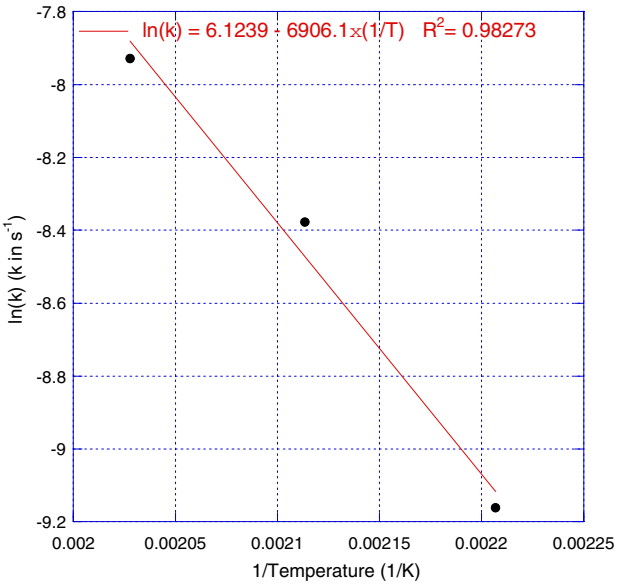

Fig. 3 Temperature dependence of the kinetic parameter k

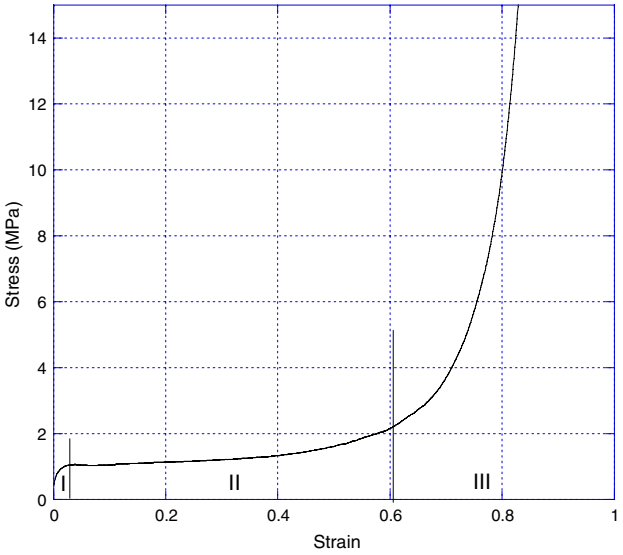

Fig. 4 A typical stress–strain curve for an underaged Duocel® foam and a schematic presentation of various deformation regimes

The stress–strain curves obtained for the aged foams at 180 and 220 °C are demonstrated in Figs. 5 and 6, respectively. For the purpose of clarity, selected aging times, and the strains up to 0.7, have been included in these figures. The results show that the levels of the so-called stress plateau [1, 20] and the yield strength increase with the increase in aging time. The yield strength values are reported in Figs. 7 and 8. It is noted that the yield strength of the solution-treated and subsequently air-quenched sample is approximately 0.5 MPa, while the peak yield strength values of approximately 1.3 and 1.1 MPa are achieved for aging of 7 h at 180 °C and 4 h at 220 °C, respectively. It should also be mentioned that samples aged for 7 h at 180 °C, 2 h at 220 °C and 4 h at 220 °C display yielding peaks and valleys on the stress–strain curves, whereas the specimens aged for shorter times at these temperatures do not display such phenomenon. The

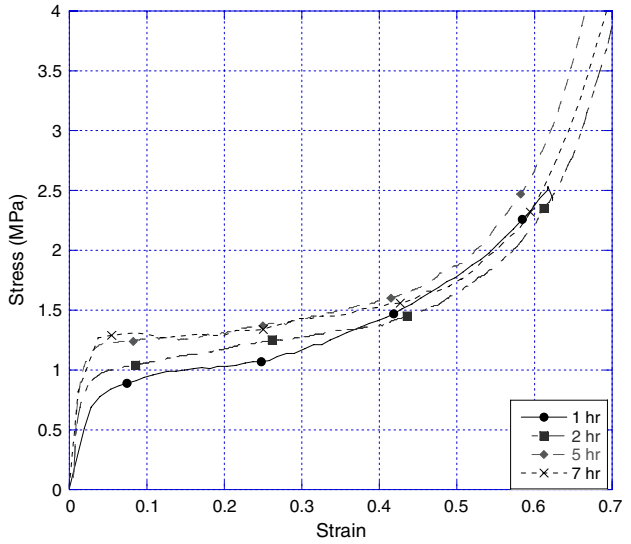

Fig. 5 Compression tests results of samples aged for various times at 180 °C

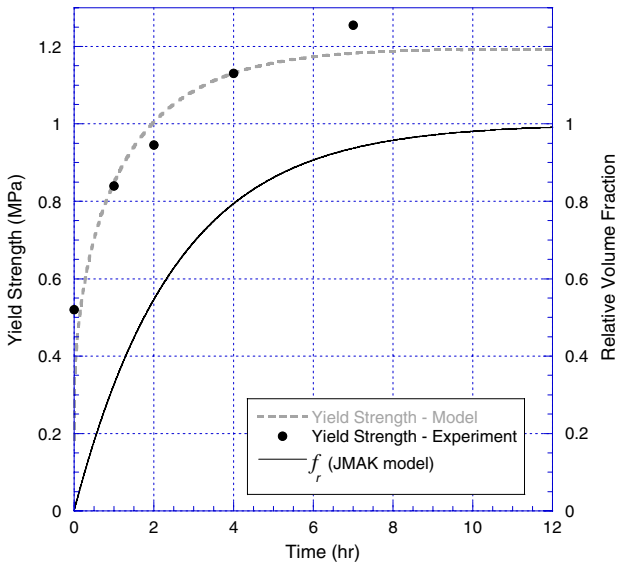

Fig. 7 The evolution of the foam yield strength and its relative volume fraction of precipitates during aging at 180 °C

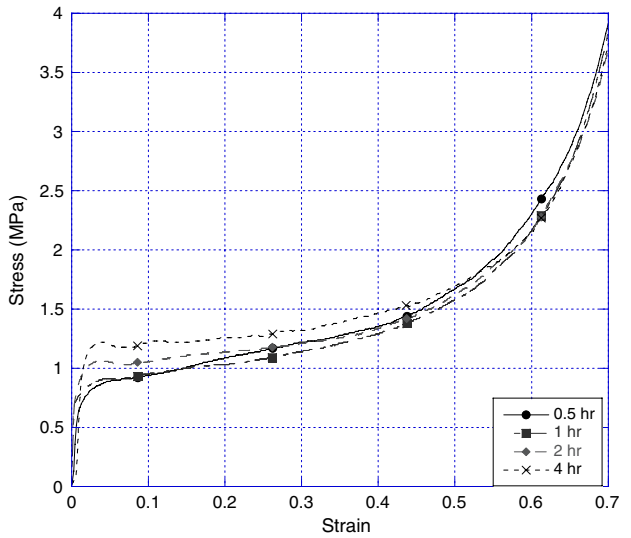

Fig. 6 Compression tests results of samples aged for various times at 220 °C

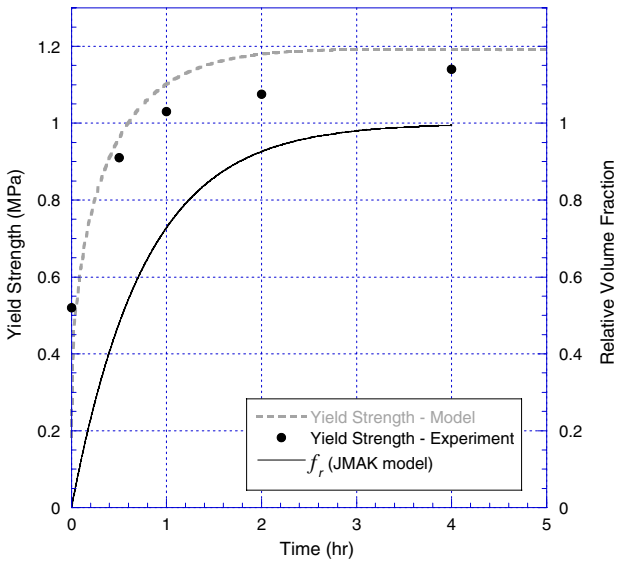

Fig. 8 The evolution of the foam yield strength and its relative volume fraction of precipitates during aging at 220 °C

stress–strain curves beyond the yield strength values are generally smooth in all cases.

Modeling of the yield strength

The yield strength of the foam is related to its relative density, as well as the yield strength of the cell wall material, according to Eq. 1. The measured relative density of the foam (i.e. $\frac{\rho^*}{\rho_s} = 0.075$) is used as the model input, while the yield strength of the cell wall material as a function of aging time at temperature is predicted using the model developed by Esmaeili et al. [22]. According to this model, the yield strength of the alloy is the linear summation of three different contributions of the intrinsic strength of pure aluminum, i.e. σ_i, the solid solution strengthening, i.e. σ_{ss}, and the precipitation strengthening, i.e. σ_{ppt}. This is presented as follows:

$$\sigma_y = \sigma_i + \sigma_{ss} + \sigma_{ppt}. \quad (5)$$

Both σ_{ss} and σ_{ppt} are functions of the extent of precipitation during aging and are given according to the following equations:

$$\sigma_{ss} = \sigma_{0ss}(1 - \alpha f_r)^{2/3} \quad (6)$$

$$\sigma_{ppt} = C_1(f_r)^{1/2} \quad (7)$$

where σ_{0ss} is solute contribution to the yield strength when the alloy is in the supersaturated solid solution (i.e. as-quenched) state. The parameter α, which represents the fraction of the initial solute content depleted from the matrix when f_r approaches unity, is assumed to be 1 [22]. C_1 is the calibration parameter that relates the precipitate strengthening at aging time t to the microstructural parameters of the peak aged alloy in the temperature range of interest [22]. The evidence for the similar precipitate content at the peak-aged condition, as discussed in Sect. "Compression testing", enables using a constant value for C_1 at the artificial aging temperatures used in this work [22]. It should be noted that Eq. 7 has been chosen to represent the precipitate strengthening assuming that the precipitates act as strong obstacles to dislocation motion. This has been reported to be the case for a number of other AA6XXX alloys for similar aging conditions [22, 24, 27].

The yield strength of the foam alloy is predicted using the modeled values for f_r and the required calibration parameters. The intrinsic strength of pure aluminum is taken as 10 MPa, while the calibration parameter σ_{0ss} is obtained based on the knowledge of the yield strength of the AA6XXX alloys in the as-quenched condition [21, 22, 24, 27, 28]. This value is assumed to be 20 MPa in the present work. The parameter C_1 is obtained based on the assumption that the yield strength of the alloy at the peak-aged condition is 193 MPa. This gives $C_1 = 183$ MPa. It should be noted that the value $\sigma_y = 193$ MPa has been provided in the ASM Handbook [23] for the T6 temper of AA6101. The interested reader is referred to reference [22] for the details of the calibration parameter estimation from the experimental yield strength values.

The foam yield strength is obtained using Eq. 1, with $C = 0.3$, and incorporating the predicted values for the yield strength of the alloy. The modeling results, along with the experimentally determined yield strength values of the heat-treated foam samples, are plotted in Figs. 7 and 8 for the aging temperatures of 180 and 220 °C, respectively. The corresponding modeled evolution of the relative volume fraction of precipitates is also included in each figure. The agreement between the modeling and experimental results for the foam yield strength is very good at both temperatures, with the variation between average experimental values and model values no larger than ±10% for the entire aging period. The sources of error in modeling results include mainly the choice of calibration parameters from the general literature data, as well as the errors related to the measurement and modeling of f_r. The comparison of the yield strength evolution during aging with the corresponding evolution of f_r shows the direct relationship between the two. In other words, a fast increase in the precipitate content during the early stages of aging corresponds to a fast increase in the yield strength of foam during aging. Similarly, the slow increase in the precipitate volume fraction when f_r approaches 1 results in leveling of the yield strength increase with aging time. Further to these observation, Figs. 7 and 8 show that the relative volume fraction of precipitates are larger than 0.9 (i.e. larger than 90%) for the aging conditions of 7 h at 180 °C, and 2 h and 4 h at 220 °C. This might explain the observation of upper yield points on the stress–strain curves for 7 h at 180 °C, and 2 h and 4 h at 220 °C, indicating a possible gradual loss of ductility as the microstructural state of the alloy approaches overaging. The above suggestion is based on the knowledge that a brittle foam produces a rough stress–strain curve and displays a distinct upper yield point followed by a drop in stress [1]. Although the present stress–strain curves are generally smooth beyond the yield point, the appearance of the upper yield point may denote some reduction in ductility. The reduction in ductility and a transition from ductile to brittle fracture mode has also been reported in an open-cell AA6061 foam after age hardening treatment of 18 h at 160 °C [19]. Further microstructural characterization and fractography of the cell walls of aged and tested samples are required to verify that loss of ductility due to overaging is the main reason for the appearance of upper yield points on the stress–strain curves.

The results of the present work suggest that the approaches adopted here provide viable tools for relatively accurate prediction of the foam strength as a function of its microstructural evolution during age hardening treatments. This is particularly of practical importance, considering that the entire microstructural characterization and modeling practices need only a small number of experiments and calibration parameters. The evidence for the gradual loss in ductility of the foam when the overaging approaches suggest that the age hardening heat treatments should be controlled to optimize the combination of mechanical properties such as strength and energy absorption capacity. The approaches adopted in this work can help to achieve the processing/property optimization goals with minimal experimental work.

Summary and conclusions

The present work has aimed at introducing a predictive tool to relate the yield strength of an open-cell AA6101 aluminum foam to its microstructural evolution during age hardening treatments. A recently developed isothermal calorimetry procedure has been used to characterize the

evolution of the volume fraction of precipitates during artificial aging in the temperature range of 180–220 °C. The kinetics of precipitation has then been formulated by fitting the so-called JMAK kinetic model to the experimentally analyzed results. The yield strength of the aged foam has been modeled by adopting the established relationship between the normalized yield strength and the relative density of the foam and the yield strength model developed for AA6XXX alloys. The results have shown that the evolution of the yield strength of the AA6101 aluminum foam during artificial aging can be predicted with an accuracy level of ±10%. The comparison of the evolution of the yield strength of foam with its corresponding microstructural evolution during aging has confirmed the direct influence of precipitation on the foam strength and its stress–strain behavior. The work has confirmed that the presented analytical and modeling approach can be effectively used to predict the strength and/or optimize processing and properties of the aged foams.

Acknowledgement The authors would like to thank the University of Waterloo and the Natural Sciences and Engineering Research Council of Canada (NSERC) for providing financial support for this investigation.

References

1. Gibson LJ, Ashby MF (1997) Cellular Solids: structure and properties, 2nd ed. Cambridge University Press, Cambridge
2. Gibson LJ (2000) Annu Rev Mater Sci 30:191
3. Banhart J (2001) Prog Mater Sci 46:559
4. Wang M, Hu X-F, Wu X-P (2006) Mater Res Bull 41:1949
5. Werther DJ, Howard AJ, Ingraham JP, Issen KA (2006) Scripta Mater 54:783
6. Lehmus D, Banhart J (2003) Mater Sci Eng A349:98
7. Gibson LJ, Ashby MF (1982) Proc R Soc Lond A382:43
8. Maiti SK, Gibson LJ, Ashby MF (1984) Acta Metall 32(11):1963
9. Despois J-F, Mueller R, Mortensen A (2006) Acta Mater 54:4129
10. Zhou J, Soboyejo WO (2004) Mater Manuf Process 19(5):863
11. Andrews E, Sanders W, Gibson LJ (1999) Mater Sci Eng A270:113
12. McCullough KYG, Fleck NA, Ashby MF (1999) Acta Mater 47(8):2323
13. Nieh TG, Higashi K, Wadsworth J (2000) Mater Sci Eng A283:105
14. Fusheng H, Zhengang Z (1999) J Mater Sci 34:291
15. Zhihua W, Hongwei M, Longmao Z, Guitong Y (2006) Scripta Mater 54:83
16. Kwon YW, Cooke RE, Park C (2003) Mater Sci Eng A343:63
17. Lehmus D, Banhart J, Rodriguez-Perez MA (2002) Mater Sci Tech 18:474
18. Lehmus D, Marschner C, Banhart J (2002) J Mater Sci 37:3447
19. Chan KC, Chan H (2004) Mater Manuf Process 19(3):407
20. Zhou J, Gao Z, Cuitino AM, Soboyejo WO (2004) Mater Sci Eng A386:118
21. Esmaeili S, Wang X, Lloyd DJ, Poole WJ (2003) Metall Mater Trans A 34A:751
22. Esmaeili S, Lloyd DJ, Poole WJ (2003) Acta Mater 51:2243
23. ASM Handbook (1990) Properties of wrought aluminum and aluminum alloys, vol 2, 10th edn. ASM International, USA, p 105
24. Esmaeili S, Lloyd DJ (2005) Acta Mater 53:5257
25. Olurin OB, Fleck NA, Ashby MF (2000) Mater Sci Eng A291:136
26. Esmaeili S (2002) Precipitation hardening behaviour of AA6111. PhD Thesis, The University of British Columbia
27. Esmaeili S, Lloyd DJ (2005) Modeling of age hardening for two variants of AlMgSi(Cu) Alloys. Light Metals 2005. Martin JP (ed) Met Soc, Montreal, Quebec, Canada, p 293
28. Esmaeili S, Lloyd DJ (2004) Scripta Mater 50:155